Malaysian Journal of Analytical Sciences (MJAS)
Published by Malaysian Analytical Sciences Society

PHYSICOCHEMICAL CHARACTERIZATION OF ZnO/G-C_3N_4 FOR PHOTO-REMOVAL OF METHYL ORANGE UNDER LOW UV-LIGHT INTENSITY

(Pencirian Fizikokimia ZnO/g-C_3N_4 untuk Penyingkiran Metil Oren di Bawah Lampu UV Berkeamatan Rendah)

Nurul Izzati Izhar[1], Zul Adlan Mohd Hir[1,2*], Hartini Ahmad Rafaie[3] and Shaari Daud[1]

[1]*Faculty of Applied Sciences, Universiti Teknologi MARA Pahang, 26400 Bandar Tun Abdul Razak Jengka, Pahang, Malaysia*
[2]*Catalysis for Sustainable Water and Energy Nexus Research Group, School of Chemical Engineering, College of Engineering, Universiti Teknologi MARA, 40450 Shah Alam, Selangor, Malaysia*
[3]*Centre of Foundation Studies, Universiti Teknologi MARA, Selangor Branch, Dengkil Campus, 43800 Dengkil, Selangor, Malaysia*

[*]*Corresponding author: zuladlan@uitm.edu.my*

Received: 14 September 2023; Accepted: 12 February 2024; Published: 29 April 2024

Abstract

UV light-active photocatalyst of ZnO/g-C_3N_4 was synthesized by a facile mixing method with different ratio of g-C_3N_4 (0.01, 0.03, 0.05, 0.07, and 0.09 g). The photocatalytic activity of ZnO/g-C_3N_4 was tested towards methyl orange (MO) dye in aqueous solution using a low UV light intensity (7W). FTIR spectroscopic results obtained show the functional groups spectrum corresponding to the ZnO and g-C_3N_4. Besides, SEM results also show the formation of heterogenous photocatalysts as irregular shape particles of ZnO interlink with g-C_3N_4 surface. EDX analysis confirms the presence of Zn, C, O, and N elements correspond to ZnO/g-C_3N_4 photocatalyst. From the results obtained, ZG3 (0.1:0.03) photocatalysts exhibit almost complete removal of methyl orange under UV irradiation in a period of 60 min (~95%). The highest degradation rate constant of 5.26×10^{-2} min^{-1}, based on pseudo-first-order kinetics is estimated. The best photocatalyst (ZG3) showed high potential in degrading MO under low UV light intensity which can be used for photocatalytic water remediation application.

Keywords: g-C_3N_4, methyl orange, photocatalysis, UV light, ZnO

Abstrak

Fotomangkin cahaya UV-aktif ZnO/g-C_3N_4 telah disintesis dengan kaedah pencampuran mudah dengan nisbah g-C_3N_4 yang berbeza (0.01 g, 0.03 g, 0.05 g, 0.07 g dan 0.09g). Aktiviti fotomangkin ZnO/g-C_3N_4 telah diuji terhadap pewarna metil oren (MO) dengan menggunakan cahaya UV berkeamatan rendah (7W). Analisa FTIR spektroskopik yang diperoleh menunjukkan spektrum kumpulan berfungsi yang sepadan dengan ZnO dan g-C_3N_4. Selain itu, analisa SEM juga menunjukkan pembentukan fotomangkin heterogen ZnO sebagai zarah bentuk tidak sekata ZnO bersaling paut dengan permukaan g-C_3N_4. Analisa EDX mengesahkan kehadiran unsur Zn, C, O dan N sepadan dengan fotomangkin ZnO/g-C_3N_4. Melalui keputusan yang diperoleh, fotomangkin ZG3 (0.1:0.03) menunjukkan penyingkiran hampir lengkap pewarna metil oren di bawah penyinaran UV dalam tempoh 60 minit (~93%). Pemalar kadar degradasi yang tertinggi adalah 5.26×10^{-2} min^{-1} berdasarkan kinetik pseudo-tertib pertama telah dianggarkan. Fotomangkin terbaik (ZG3) menunjukkan potensi yang tinggi untuk degradasi MO dibawah keamatan cahaya UV

yang rendah yang boleh digunakan untuk aplikasi pemulihan air fotomangkin.

Kata kunci: g-C_3N_4, metil oren, fotokatalisis, cahaya UV, ZnO

Introduction

Since the last few decades, industrialization, technologies, and consumption of non-renewable resources have grown at a rapid pace, owing to the constant increase in demand for textile, dye, fertilizer, domestic, and plastic materials. As a result, environmental pollution and energy crises have already reached alarming proportions. Industrial wastes are more toxic and nonbiodegradable than municipal wastes because they contain fats, oil, grease, heavy metals, phenols, and ammonia, among other things [1]. The negative effects of these pollutants on human and wildlife reproductive health have become a major source of public concern [2]. Though since traditional wastewater treatment methods aren't designed to remove toxic organic pollutants, these toxins have ended up in aquatic life, where they can subsequently make their way into the human food chain [3].

In the fight against the accumulation of organic wastes in the environment and aquatic life, heterogeneous semiconductor photocatalysis has been proposed as an effective method of removing this pollution. Zinc oxide (ZnO) is a semiconductor metal oxide and widely regarded as the most potential photocatalytic materials for the abatement of pollutant in water. It has a wide bandgap of 3.37 eV, good mechanical, thermal, and chemical stability, nontoxic, cost-efficient, and can also absorb a large portion of the light spectrum (UV/solar) [4–6]. However, the photo-corrosion of pure ZnO caused by the photoinduced holes is found to be severe during the reaction, which could affect the stability and photocatalytic activity of ZnO [7]. Furthermore, the rapid recombination of photoinduced electrons and holes limits its practical application due to its weak photocatalytic activity. Several initiatives, such as metal doping, have been made to enhance its charge separation efficiency and prevent photo-corrosion [8], as well as non-metal doping [9], and heterojunction formation [10].

Recently, graphitic carbon nitride (g-C_3N_4) has proved to be a promising candidate to form heterojunctions with ZnO [11, 12]. The material in question is a metal-free, n-type polymeric semiconductor with a narrow bandgap of 2.7 eV that could provide a viable solution to increase charge separation [13]. Previous research has revealed that the heterostructure formation and synergistic interaction between ZnO and g-C_3N_4 continue to improve photocatalytic activity. Ismael, for example, synthesized ZnO/g-C_3N_4 using a simple calcination process, and the photocatalytic enhancement was attributed to an increase in the quantity of the surface hydroxyl group [11]. Alternately, Le et al. synthesized ZnO/mesoporous g-C_3N_4 using a hard-templating technique, which then discovered that those composite photocatalysts exhibited remarkable photocatalytic activity due to effective charge carrier separation at the heterojunction interfaces [14]. The charge recombination rate can be reduced with an appropriate band alignment, resulting in improved high electron transfer and increased photocatalytic activity. However, not many studies proposed the photocatalytic activity of ZnO through n-n heterojunction with g-C_3N_4 under low UV light intensity. Accordingly, an improved surface area and visible light absorption capacity of the g-C_3N_4-ZnO composite resulted in more active sites, photogenerated electron-hole pairs, and a lower frequency of photo-induced charge recombination, all of which improved the photoactivity potential [12]. On the other hand, the band adjustment at the interface was responsible for the type-II heterojunction formation and the subsequent charge transfer process from g-C_3N_4 to ZnO at the interface [15]. Direct addition of g-C_3N_4 to ZnO nanocomposite results in a decrease in crystalline size, an increase in optical bandgap, and a modification in nanocomposite morphology. When compared to pure ZnO, g-C_3N_4 significantly improves the photocatalytic performance of g-C_3N_4@ZnO nanocomposites under visible light irradiation [16].

In this work, ZnO/g-C_3N_4 composite photocatalysts were synthesized by a simple mixing approach with the use of commercially available ZnO and dicyanamide as the precursor for g-C_3N_4. By only changing the mass of g-C_3N_4, a variety of composites with various ratios were created. Utilizing X-ray diffraction (XRD), scanning

electron microscopy (SEM), energy dispersive spectroscopy (EDX), and Fourier transform infrared (FTIR), we looked at the structural, morphological, surface compositions, and functional groups of the ZnO/g-C_3N_4 photocatalysts. In order to assess the photocatalytic activity of ZnO/g-C_3N_4 under low UV light intensity (7 W), the probe molecule methyl orange (MO) dye was chosen. Grafting of non-metal materials like g-C_3N_4 onto a wide bandgap ZnO photocatalyst could be an alternative strategy to prepare a stable and efficient photocatalyst for water remediation process.

Materials and Methods

Materials

Commercial zinc oxide (ZnO, 99%) and dicyanamide ($C_2H_4N_4$, 99%) were purchased from Sigma-Aldrich (Selangor, Malaysia). Methyl orange dye was obtained from Bendosen Laboratory Chemicals (Selangor, Malaysia). All chemicals were used as received and deionized water was used throughout the experimental procedures.

Preparation of g-C_3N_4

Dicyandiamide (0.1 mol) was dissolved in a deionized water (50 mL) and magnetically stirred for 1 hour. Next, the solution was dried in the oven at 80 °C overnight, followed by calcination in a muffle furnace at 500 °C for 2 hours (heating rate: 5°C/min) in a close crucible. The obtained yellow powder of g-C_3N_4 was grounded and stored for later use.

Preparation of ZnO/g-C_3N_4 composite photocatalyst

ZnO/g-C_3N_4 composite photocatalyst was prepared by mixing the two materials through different mass ratios of g-C_3N_4. First, 0.01g of previously prepared g-C_3N_4 was mixed with 0.10g ZnO and dispersed in a deionized water (50 mL) with continuous stirring for 1 h. The collected light-yellow sample was dried in the oven at 80 °C overnight and labelled as ZG1. The same procedure was repeated with different masses of g-C_3N_4. The composition of the prepared photocatalysts is presented in Table 1.

Table 1. Compositions for the preparation of ZnO/g-C_3N_4

Photocatalyst	ZnO (g)	g-C_3N_4 (g)
ZG1	0.10	0.01
ZG3	0.10	0.03
ZG5	0.10	0.05
ZG7	0.10	0.07
ZG9	0.10	0.09

Physicochemical characterization of ZnO/g-C_3N_4 composite photocatalyst

The XRD patterns were recorded using a powder X-ray diffractometer (XRD6000, Shimadzu) with Cu Kα radiation (λ = 1.540 Å, 30 kV, and 30 mA) in the 2θ range of 10–70° with a scanning speed of 2°/min. The structural and elemental compositions were characterized using a scanning electron microscope equipped with an electron dispersive X-ray analyzer (SEM-EDX, TESCAN VEGA3). The presence of functional groups in the ZnO/g-C_3N_4 photocatalysts were analyzed by Fourier transform infrared (FT-IR) between 4000 to 500 cm^{-1} on a Perkin Elmer Infrared Spectrometer.

Photocatalytic evaluation of ZnO/g- C_3N_4 composite photocatalyst

The calibration plot of the selected pollutant methyl orange (MO) dye in aqueous solution under normal condition was carried out prior to the photocatalytic activity. The calibration curve was plotted based on different concentrations of the selected pollutant ranging from 5 to 25 mg/L. The linear equation was calculated from this calibration plot by measuring the absorbance of each sample at maximum wavelength (λ_{max} = 464 nm). Figure 1 shows the photodegradation of methyl orange in aqueous solution in a 250 mL glass photoreactor with a low intensity of UV-C light (7 W). A preliminary test which is photolysis was done on MO without the addition of photocatalyst to determine that no degradation of MO occurs when irradiated with low-intensity UV light. The system received a predetermined

amount of the powder photocatalyst. To assure the presence of dissolved oxygen in the solution, the photoreactor was then constantly supplied with air at a flow rate of 4 L/min. First, the working solution was agitated for 30 minutes in the absence of light to achieve adsorption-desorption equilibrium. The solution was then exposed to UV light for 60 minutes while being continuously stirred. The liquid (5-10 mL) was collected at predefined time intervals and filtered to remove the photocatalyst and the concentration left was monitored using a Perkin Elmer UV–vis spectroscopy (UV-2550, Shimadzu). In this study, the percentage of degradation was calculated using Equation (1) [17].

$$\text{Percentage of degradation (\%)} = \left[\frac{(C_t - C_0)}{C_0}\right] X\ 100\% \quad (1)$$

where C_o is the concentration of pollutant before irradiation and C_t is the concentration of pollutant at 't' min.

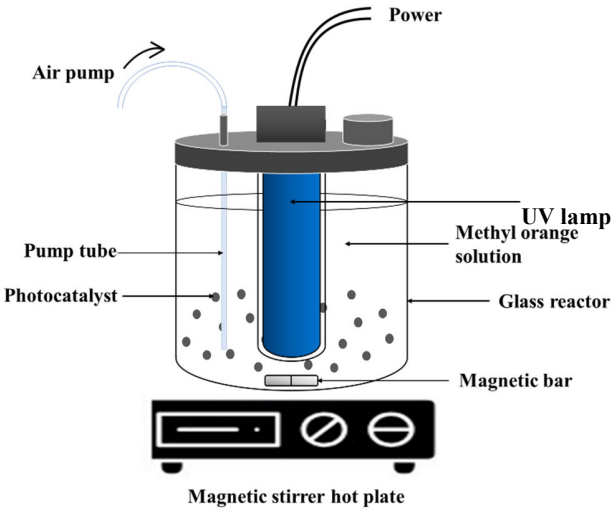

Figure 1. Schematic illustration of photoreactor set up for degradation of MO dye in aqueous solution using ZnO/g-C_3N_4 composite photocatalyst

The kinetics of the MO degradation by the prepared photocatalysts was studied based on the Langmuir–Hinshelwood (L–H) kinetic model using the following equation:

$$r = \left(\frac{dC}{dt}\right) = k_{obs}C \quad (2)$$

which can be rewritten as

$$ln\left(\frac{C_o}{C_t}\right) = k_{obs}t \quad (3)$$

where r is the reaction rate, k_{obs} is the rate constant (min^{-1}), and C_o and C_t are the concentration (mg/L) of MO initially and at different irradiation times, respectively.

Results and Discussion

Physicochemical characterization of ZnO/g-C_3N_4 composite photocatalyst: XRD analysis

The XRD patterns of pure g-C_3N_4, pure ZnO, and ZnO/g-C_3N_4 composite photocatalysts are shown in Figure 2. The pure g-C_3N_4 pattern (Figure 2a) shows some peaks as the (002) lattice planes' most strong peak, which corresponds to the interplanar stacking peak of conjugated aromatic rings, is identified at 28.16° [18–20]. The peak of 13.27° locates (100) lattice plane attributed to the in-plane structural repeating unit of N-bridged tri-s-triazine [18, 21]. In the meantime, ZnO's typical diffraction peaks are found at 31.78°, 34.40°, 36.25°, 47.54°, 56.58°, 62.82°, 67.94°, and 69.04°, with corresponding crystal indices of (100), (002), (101), (102), (110), (103), (200), (112), (201), and (202)

(Figure 2b), indicating that ZnO is the wurtzite as confirmed from the standard (JCPDS card 36–1451) [22, 23]. Next, the samples of ZG composite photocatalysts exhibit associated diffraction peaks for ZnO and g-C_3N_4 (Figure 2c-g). The presence of g-C_3N_4 diffraction peaks becomes more noticeable as the content of g-C_3N_4 was increased up to 0.09 g. It can be clearly observed that the ZG7 and ZG9 composite exhibits two-phase compositions of both ZnO and g-C_3N_4, as demonstrated by their diffraction peaks and the absence of any further peaks (Figure 2f and g). Comparing all composite photocatalysts to pure ZnO and pure g-C_3N_4, the positions of the distinctive peaks are often unchanged. This demonstrates that the ZnO/g-C_3N_4 combination has no effect on the stability of the lattice structures of individual ZnO and g-C_3N_4 [24].

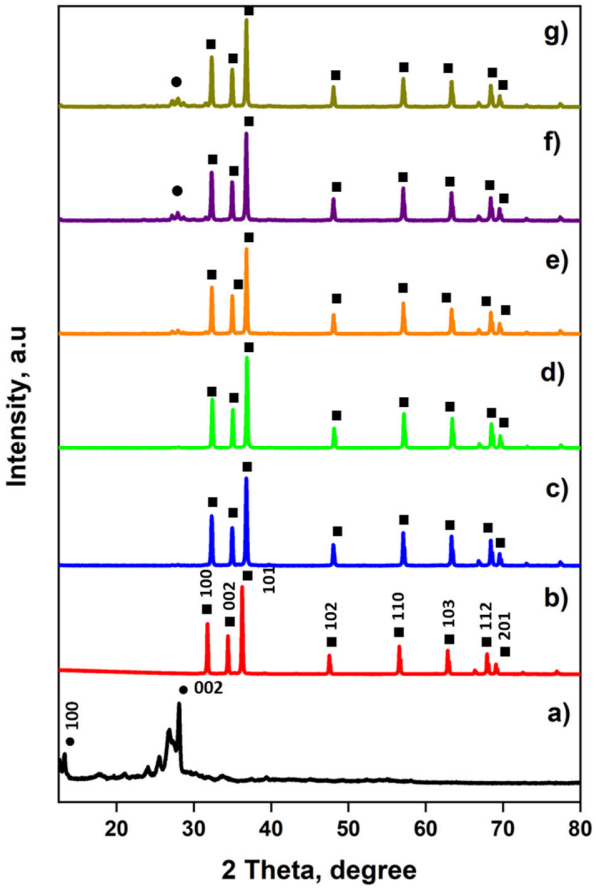

Figure 2. XRD patterns of a) pure g-C_3N_4, b) pure ZnO, c) ZG1, d) ZG3, e) ZG5, f) ZG7 and g) ZG9 photocatalysts

SEM-EDX analysis

Scanning electron microscopy (SEM) was used to examine the morphology of the prepared photocatalysts. At a magnification of 2000x, the photocatalyst images are noticed. The SEM morphology for pure ZnO, pure g-C_3N_4, and ZnO/g-C_3N_4 composite photocatalysts with various ratio compositions are shown in Figure 3. Pure ZnO reveals that it is made up of agglomerated and irregularly shaped particles (Figure 3a). It was previously reported that pure g-C_3N_4 depicted shape of irregular sheet-like meanwhile other researcher reported that pure g-C_3N_4 showed layered morphology and this is consistent with the results obtained in this study; pure g-C3N4 has a sheet-like surface and layered structure (Figure 3b) [25, 26]. Figure 3c)–d) depicts the morphology of ZnO/g-C_3N_4 composites with various g-C_3N_4 compositions. Figure 3c-g shows that ZnO are dispersed across the graphitic carbon nitride (g-C_3N_4)

surface, which helps the two phases form a heterojunction, improving charge transfer and separation as well as the photocatalytic activity of the composites [27]. This demonstrates the interactions between ZnO and g-C_3N_4 at the interface, which could help with internal electron migration to the photocatalyst surface and the effective separation of photoinduced excited photons [26].

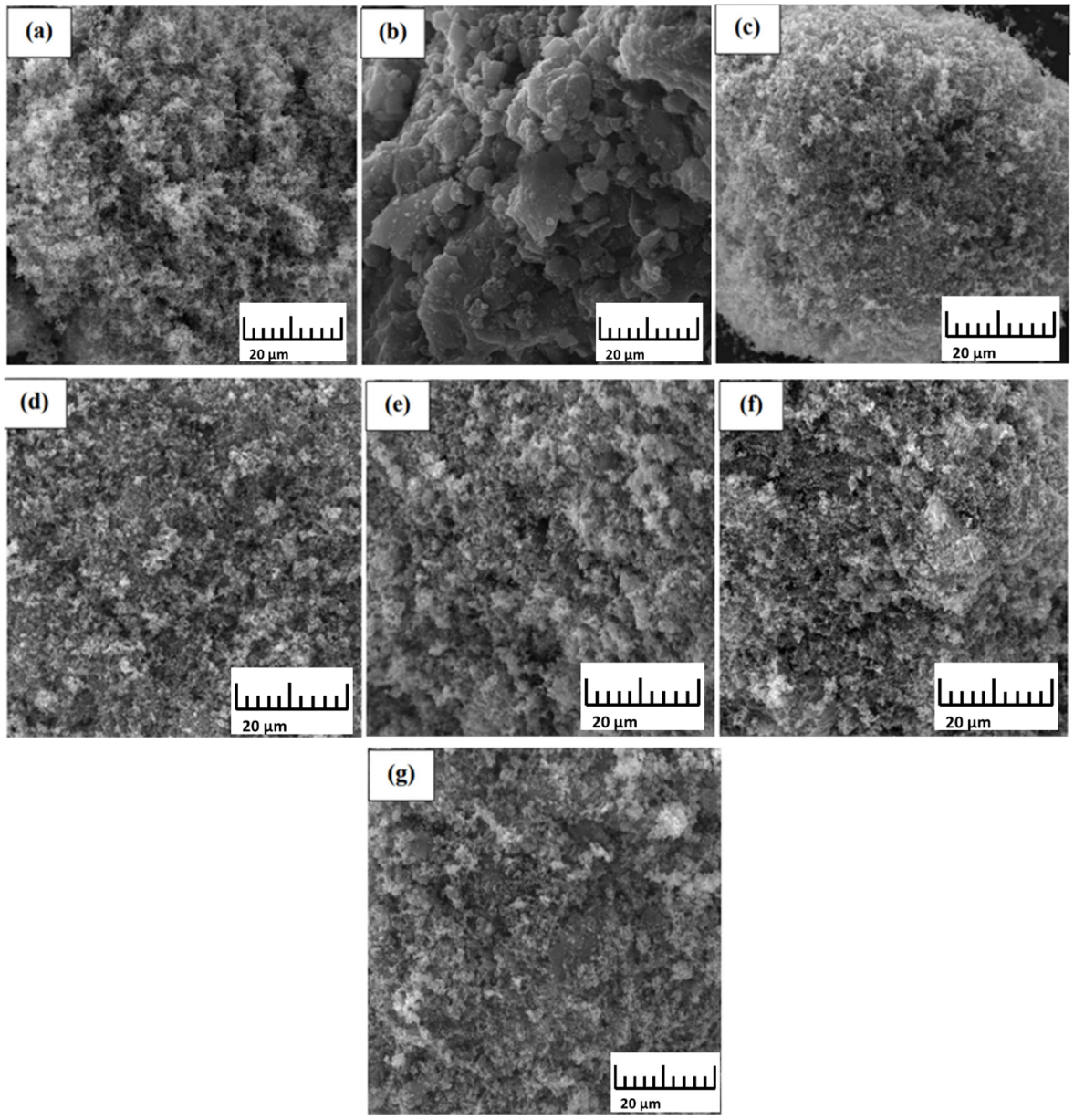

Figure 3. SEM images of (a) pure ZnO, (b) pure g-C_3N_4, (c) ZG1, (d) ZG3, (e) ZG5, (f) ZG7, and (g) ZG9

The EDX study was conducted to support the results from the SEM examination and to further confirm the presence of ZnO and g-C_3N_4 in the ZnO/g-C_3N_4 composite photocatalyst. The existence of zinc, carbon, oxygen, and nitrogen has been established for the ZG1 and ZG9 photocatalyst, confirming the composition of ZnO/g-C_3N_4, as illustrated in Figure 4a) and 4b) below.

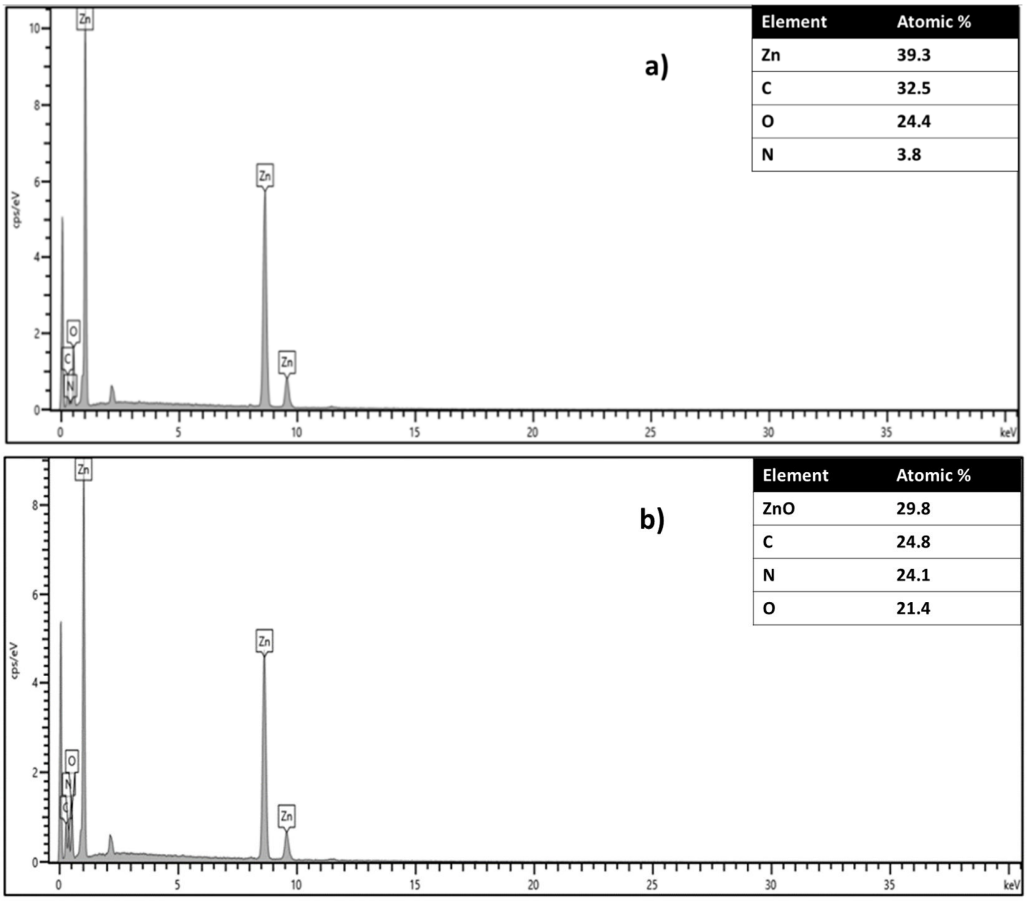

Figure 4. EDX analysis of a) ZG1, and b) ZG9

FTIR analysis

The distinct functional groups and chemical bonds present in the pure ZnO, pure g-C_3N_4, and ZnO/g-C_3N_4 composite photocatalysts were determined using the Fourier transform infrared spectroscopy (FTIR) analysis (Figure 5). From the spectrum, Zn-O bond vibrational modes can be detected in the band at the 560.80 cm^{-1} region. It is also possible to see a peak at 3348.90 cm^{-1}, which indicates the existence of a hydroxyl group in the ZnO component resulting from water molecules adhering to the oxide's surface [28]. The prepared g-C_3N_4 exhibits peaks between 1240 and 1640 cm^{-1} that indicates the presence of C_3N_4 heterocycle stretching modes. While aromatic C-N stretching vibration modes are responsible for the peak at 1463.47 cm^{-1}, C=N stretching is represented by the peak at 1613.81 cm^{-1} [29]. The triazine units of g-C_3N_4 have out-of-plane bending vibration modes that are associated to the peak at 797.32 cm^{-1} area [12]. Additionally, the N-H stretching modes are responsible for the absorption peak at 3098.56 cm^{-1}, which is between 2900 and 3400 cm^{-1} [15]. The spectrum of the ZnO/g-C_3N_4 composite photocatalyst are similar to the main peaks of g-C_3N_4, indicating that the component's structure was preserved even after combining with ZnO (subset a) and b) of Figure 5). Plus, the characteristics peaks of ZnO can also be seen in the spectrum because of its high content in the photocatalyst (subset c) of Figure 5). Moreover, the conjugated system of the g-C_3N_4 is stretched because the band red-shifted and the band strengths also diminished [30]. Thus, a broader conjugated system is generated between the ZnO and g-C_3N_4 [30]. The interfacial interaction between the ZnO and g-C_3N_4 will improve the photocatalytic performance as it will enable the transportation of photoinduced charges [26].

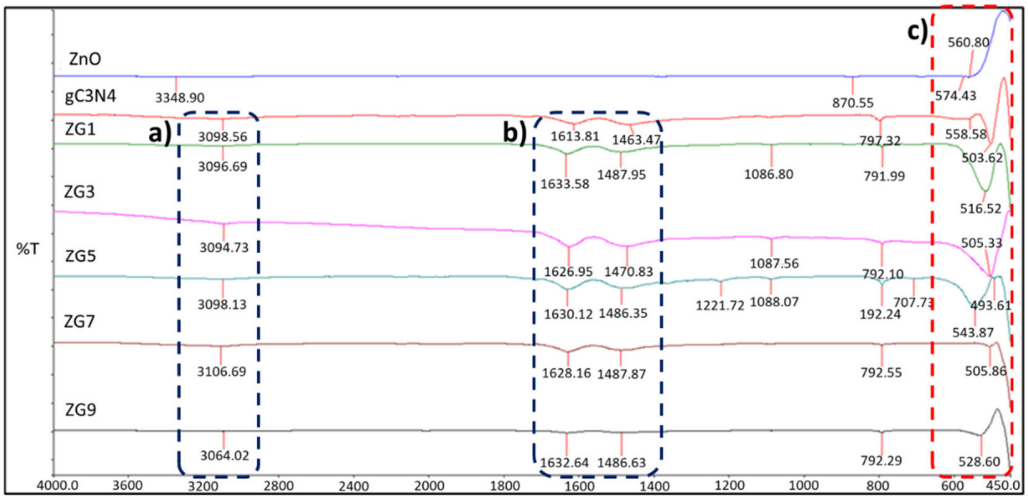

Figure 5. FTIR spectra of all prepared photocatalysts

Photocatalytic performance of ZnO/g-C_3N_4 photocatalyst

The photocatalytic degradation of MO dye by pure ZnO, pure g-C_3N_4, and ZnO/g-C_3N_4 composite photocatalysts with varied mass ratios is shown in Figure 6a). According to preliminary investigations, no degradation of MO was found throughout the photolysis process, indicating that MO was stable against UV light irradiation, with a negligible effect. In 60 minutes, pure ZnO shows 2.2 times the percentage of degradation greater than pure g-C_3N_4 (33%). In degrading MO, all generated ZnO/g-C_3N_4 composite photocatalysts demonstrate a higher percentage of degradation than pure ZnO (Figure 5a). Interestingly, with a maximum percentage of degradation of 95%, the ZG3 photocatalyst with a ratio of 0.1:0.03 is shown to be the best. It can be seen that the photocatalytic activity and degradation rate increase with an increasing amount of g-C_3N_4 up to 0.03g. As previously reported, the heterojunction that formed between ZnO and g-C3N4 is what led to the improved photocatalytic activity [11], [31–33]. However, as the g-C_3N_4 percentage increase (> 0.03), the photocatalytic activity and degradation rate falls dramatically due to the presence of aggregated particles, which lowers the surface area and light absorption capacity of the composite photocatalysts. When subjected to UV light, the photocatalyst may not function as well due to the reduced capacity of the photoinduced electrons to transfer electrons from ZnO to the g-C_3N_4 surface [34]. These results reveal the fact that there is a limitation to the amount of g-C_3N_4 that can be integrated into the ZnO surface without negatively impacting the percentage of degradation and the rate of deterioration. Therefore, ZG3 contains the appropriate ratio for the degradation of MO dye when exposed to low intensity of UV light irradiation. Given the strong synergistic interactions between ZnO and g-C_3N_4, it is clear that both elements are crucial for the enhanced photocatalytic activity.

As depicted in Figure 6b), the degradation of MO follows pseudo first-order kinetics. Likewise, the degradation percentage, the ZG3 has the greatest rate constant of 5.26 x 10^{-2} min^{-1} and, as a result, the highest rate of MO deterioration. Table 2 shows the degradation percentage and pseudo first-order kinetics for all produced photocatalysts.

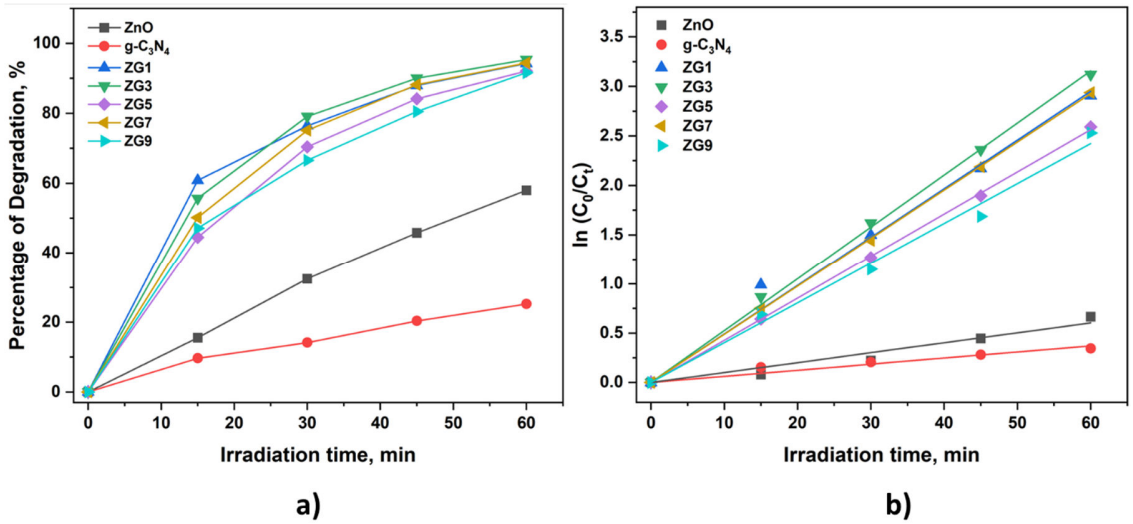

Figure 6. a) Degradation percentages and b) kinetics of the degradation of MO by all prepared photocatalysts

Table 2. Percentage of degradation and pseudo first-order kinetic for all prepared photocatalysts

Photocatalyst	Percentage of Degradation (%)	Rate Constant, K_{obs} (min^{-1}) × 10^{-2}	Rate (mg/L ·min)	Correlation Factor, R^2
Pure ZnO	57.97	1.01	0.1038	0.9782
Pure g-C_3N_4	25.20	0.62	0.0637	0.9809
ZG1	94.23	4.92	0.5057	0.9958
ZG3	95.35	5.26	0.5407	0.9995
ZG5	92.10	4.27	0.4389	0.9999
ZG7	94.41	4.88	0.5016	0.9999
ZG9	91.60	4.04	0.4153	0.9964

Conclusion

A simple mixing method was used to prepare the ZnO/g-C_3N_4 composite photocatalyst, resulting in an efficient photocatalytic removal of methyl orange (MO) dye under low UV light intensity. The findings demonstrate that the synthesized photocatalysts showed aggregated semi-spherical ZnO particles interlink with g-C_3N_4 surface. This can aid in achieving effective charge separation and lowering the rate of recombination of photoinduced charge carriers. Since ZG3 had the best photocatalytic performance which displayed ~95% photodegradation efficiency in a period of 60 min compared to other photocatalysts, it had the optimal ratio of ZnO and g-C_3N_4 contents. Overall, this research not only offers a different approach to construct ZnO/g-C_3N_4 photocatalysts through heterostructure synthesis, but also encourages simple and inexpensive processing methods.

Acknowledgements

The authors would like to thank the Ministry of Higher Education (MOHE) for financial supports under the Fundamental Research Grant Scheme (FRGS) (Project Number: FRGS/1/2021/STG05/UITM/02/17), Turn Thesis to Paper Research Grant (GT2P)(Project Number: 600-TNCPI 5/3/DDN (06) (014/2023), Universiti Teknologi MARA (UiTM) Pahang and UiTM Shah Alam for the services and facilities to carry out the laboratory work.

References

1. Mutamim, N. S. A., Noor, Z. Z., Hassan, M. A. A.,

and Olsson, G. (2012). Application of membrane bioreactor technology in treating high strength industrial wastewater: a performance review. *Desalination,* 305: 1-11.

2. Ohore, O. E., and Zhang, S. (2019). Endocrine disrupting effects of bisphenol A exposure and recent advances on its removal by water treatment systems. A review. *Scientific African,* 5: e00135.
3. Balabanič, D., Rupnik, M. and Klemenčič, A. K. (2011). Negative impact of endocrine-disrupting compounds on human reproductive health. *Reproduction, Fertility and Development,* 23(3): 403-416.
4. Kumar, S., Dhiman, A., Sudhagar, P., and Krishnan, V. (2018). ZnO-graphene quantum dots heterojunctions for natural sunlight-driven photocatalytic environmental remediation. *Applied Surface Science,* 447: 802-815.
5. Qi, K., Cheng, B., Yu, J., and Ho, W. (2017). Review on the improvement of the photocatalytic and antibacterial activities of ZnO. *Journal of Alloys and Compounds,* 727: 792-820.
6. Pullagurala, V. L. R., Adisa, I. O., Rawat, S., Kim, B., Barrios, A. C., Medina-Velo, I. A., ... and Gardea-Torresdey, J. L. (2018). Finding the conditions for the beneficial use of ZnO nanoparticles towards plants-A review. *Environmental Pollution,* 241: 1175-1181.
7. Zhou, J., Zhang, M., and Zhu, Y. (2014). Preparation of visible light-driven gC 3 N 4@ ZnO hybrid photocatalyst via mechanochemistry. *Physical Chemistry Chemical Physics,* 16(33): 17627-17633.
8. Rafaie, H. A., Nor, R. M., Azmina, M. S., Ramli, N. I. T., and Mohamed, R. (2017). Decoration of ZnO microstructures with Ag nanoparticles enhanced the catalytic photodegradation of methylene blue dye. *Journal of Environmental Chemical Engineering,* 5(4): 3963-3972.
9. Roza, L., Fauzia, V., Rahman, M. Y. A., Isnaeni, I., and Putro, P. A. (2020). ZnO nanorods decorated with carbon nanodots and its metal doping as efficient photocatalyst for degradation of methyl blue solution. *Optical Materials,* 109: 110360.
10. Mousa, H. M., Alenezi, J. F., Mohamed, I. M., Yasin, A. S., Hashem, A. F. M., and Abdal-Hay, A. (2021). Synthesis of TiO_2@ ZnO heterojunction for dye photodegradation and wastewater treatment. J*ournal of Alloys and Compounds,* 886: 161169.
11. Ismael, M. (2020). The photocatalytic performance of the ZnO/g-C_3N_4 composite photocatalyst toward degradation of organic pollutants and its inactivity toward hydrogen evolution: the influence of light irradiation and charge transfer. *Chemical Physics Letters,* 739: 136992.
12. Paul, D. R., Gautam, S., Panchal, P., Nehra, S. P., Choudhary, P., and Sharma, A. (2020). ZnO-modified g-C_3N_4: a potential photocatalyst for environmental application. *ACS Omega*, 5(8): 3828-3838.
13. Mukhair, H., Abdullah, A. H., Hir, Z. A. M., Osman, N. S., Zainal, Z., and Ngee, L. H. (2023). In-depth investigation on the photostability and charge separation mechanism of Ag_3PO_4/g-C_3N_4 photocatalyst towards very low visible light intensity. *Journal of Molecular Liquids,* 376: 121494.
14. Le, S., Jiang, T., Li, Y., Zhao, Q., Li, Y., Fang, W., and Gong, M. (2017). Highly efficient visible-light-driven mesoporous graphitic carbon nitride/ZnO nanocomposite photocatalysts. *Applied Catalysis B: Environmental,* 200: 601-610.
15. Bayan, S., Gogurla, N., Midya, A., and Ray, S. K. (2016). White light emission characteristics of two dimensional graphitic carbon nitride and ZnO nanorod hybrid heterojunctions. *Carbon,* 108: 335-342.
16. Luu Thi, L. A., Neto, M. M., Van, T. P., Nguyen Ngoc, T., Nguyen Thi, T. M., Nguyen, X. S., and Nguyen, C. T. (2021). In situ g-C_3N_4@ ZnO nanocomposite: one-pot hydrothermal synthesis and photocatalytic performance under visible light irradiation. *Advances in Materials Science and Engineering,* 2021: 1-10.
17. Hir, Z. A. M., Alam, N. M. F. H. N. B., Shaari, A. S., and Rafaie, H. A. (2022). One-pot sol-gel synthesis of a zinc oxide-reduced graphene oxide composite: Photocatalysis and kinetics studies using a fuzzy inference system. *Malaysian Journal Chemistry,* 24(2): 37-46.
18. Zhao, Z., Wang, X., Shu, Z., Zhou, J., Li, T., Wang, W., and Tan, Y. (2018). Facile preparation of

hollow-nanosphere based mesoporous g-C3N4 for highly enhanced visible-light-driven photocatalytic hydrogen evolution. *Applied Surface Science,* 455: 591-598.

19. Si, Y., Sun, Z., Huang, L., Chen, M., and Wu, L. (2019). A "ship-in-a-bottle" strategy to fabricate highly crystallized nanoporous graphitic C_3N_4 microspheres under pressurized conditions. *Journal of Materials Chemistry A*, 7(15): 8952-8959.
20. Li, Y., Yang, M., Xing, Y., Liu, X., Yang, Y., Wang, X., and Song, S. (2017). Preparation of carbon-rich g-C_3N4 nanosheets with enhanced visible light utilization for efficient photocatalytic hydrogen production. *Small,* 13(33): 1701552.
21. Lia, J., Wang, Y., Li, X., GaO, Q., and Zhang, S. (2021). A facile synthesis of high-crystalline g-C_3N_4 nanosheets with closed self-assembly strategy for enhanced photocatalytic H_2 evolution. *Journal Alloys Compounds*, 881: 1-9.
22. Cai, J., Zhang, A., Tao, H., Li, R., Han, J., and Huang, M. (2022). In situ growth TiO_2 nanoparticles on mxene (Ti_3C_2) decorated with nio quantum dots for enhanced photocatalytic performance. *SSRN*, 2022: 4045349.
23. Chen, Z., Fang, Y., Wang, L., Chen, X., Lin, W., and Wang, X. (2021). Remarkable oxygen evolution by Co-doped ZnO nanorods and visible light. *Applied Catalysis B: Environmental,* 296: 120369.
24. Li, L., Sun, S. Q., Wang, Y. X., and Wang, C. Y. (2018). Facile synthesis of ZnO/g-C_3N_4 composites with honeycomb-like structure by H_2 bubble templates and their enhanced visible light photocatalytic performance. *Journal of photochemistry and photobiology A: Chemistry*, 355: 16-24.
25. Ma, X., Huo, X., Hao, K., Song, L., Yu, Q., Liu, T., and Wang, Z. (2021). Visible light driven VO_2/g-C_3N_4 Z-scheme composite photocatalysts for selective oxidation of DL-1-phenylethyl alcohol under Vis-LEDs irradiation and aerobic oxidation. *ChemistrySelect,* 6(9): 2101-2110.
26. Alfaifi, M. Q. and Bagabas, A. A. (2019). Preparation, characterization, and application in water purification of gC_3N_4/I-TiO_2 composite photocatalysts. *Advance Material Sciences,* 4: 1-10.
27. Ismael, M. (2020). The photocatalytic performance of the ZnO/g-C_3N_4 composite photocatalyst toward degradation of organic pollutants and its inactivity toward hydrogen evolution: the influence of light irradiation and charge transfer. *Chemical Physics Letters,* 739: 136992.
28. Goulart, L. A., Alves, S. A., and Mascaro, L. H. (2019). Photoelectrochemical degradation of bisphenol A using Cu doped WO_3 electrodes. *Journal of Electroanalytical Chemistry,* 839: 123-133.
29. Brasileiro, I. L. O., Madeira, V. S., Lopes-Moriyama, A. L., and de Almeida Ramalho, M. L. R. (2023). Addition of g-C_3N_4 to ZnO and $ZnFe_2O_4$ to improve photocatalytic degradation of emerging organic pollutants. *Ceramics International,* 49(3): 4449-4459.
30. Zhu, Y. P., Li, M., Liu, Y. L., Ren, T. Z., and Yuan, Z. Y. (2014). Carbon-doped ZnO hybridized homogeneously with graphitic carbon nitride nanocomposites for photocatalysis. *The Journal of Physical Chemistry C*, 118(20): 10963-10971.
31. Sundaram, I. M., Kalimuthu, S., and Ponniah, G. (2017). Highly active ZnO modified g-C_3N_4 nanocomposite for dye degradation under UV and visible light with enhanced stability and antimicrobial activity. *Composites Communications,* 5: 64-71.
32. Yang, P., Wang, J., Yue, G., Yang, R., Zhao, P., Yang, L., ... and Astruc, D. (2020). Constructing mesoporous g-C_3N_4/ZnO nanosheets catalyst for enhanced visible-light driven photocatalytic activity. *Journal of Photochemistry and Photobiology A: Chemistry,* 388: 112169.
33. Garg, R., Gupta, R., and Bansal, A. (2021). Synthesis of g-C_3N_4/ZnO nanocomposite for photocatalytic degradation of a refractory organic endocrine disrupter. *Materials Today: Proceedings,* 44: 855-859.
34. Sun, J. X., Yuan, Y. P., Qiu, L. G., Jiang, X., Xie, A. J., Shen, Y. H. and Zhu, J. F. (2012). Fabrication of composite photocatalyst gC_3N_4–ZnO and enhancement of photocatalytic activity under visible light. *Dalton Transactions,* 41(22): 6756-6763.